Chemical Science

ROYAL SOCIETY OF CHEMISTRY

EDGE ARTICLE

View Article Online
View Journal | View Issue

Cite this: *Chem. Sci.*, 2022, **13**, 9305

All publication charges for this article have been paid for by the Royal Society of Chemistry

Received 27th April 2022
Accepted 15th July 2022

DOI: 10.1039/d2sc02365b

rsc.li/chemical-science

Three-dimensional microporous and mesoporous covalent organic frameworks based on cubic building units†

Li Liao, Xinyu Guan, Haorui Zheng, Zerong Zhang, Yaozu Liu, Hui Li,* Liangkui Zhu, Shilun Qiu, Xiangdong Yao* and Qianrong Fang *

Covalent organic frameworks (COFs) have attracted extensive interest due to their unique structures and various applications. However, structural diversities are still limited, which greatly restricts the development of COF materials. Herein, we report two unusual cubic (8-connected) building units and their derived 3D imine-linked COFs with **bcu** nets, JUC-588 and JUC-589. Owing to these unique building blocks with different sizes, the obtained COFs can be tuned to be microporous or mesoporous structures with high surface areas (2728 $m^2\ g^{-1}$ for JUC-588 and 2482 $m^2\ g^{-1}$ for JUC-589) and promising thermal and chemical stabilities. Furthermore, the high selectivity of CO_2/N_2 and CO_2/CH_4, excellent H_2 uptakes, and efficient dye adsorption are observed. This research thus provides a general strategy for constructing stable 3D COF architectures with adjustable pores *via* improving the valency of rigid building blocks.

Introduction

Constructed from organic building blocks and dynamic covalent linkages, covalent organic frameworks (COFs)[1–5] have been widely studied in gas adsorption,[6–8] heterogeneous catalysis,[9–15] energy storage,[16–20] and many other fields.[21–26] Highly designable structures, light element compositions, large surface areas and promising stabilities endow these materials with prominent performances and potential applications.[27–29] Interestingly, nano-morphologies of COFs, such as thin films and nanospheres, have also been explored and showed promising properties.[30–35] Different from the common two-dimensional (2D) species, three-dimensional (3D) COFs are still scarce due to the limited building blocks and the serious crystallization problem. To date, only about a dozen of 3D topologies are available in the COF library, while most of them are based on 3- or 4-connected knots.[36] Recently, several high valency knots have been designed successfully.[37] For example, Cooper *et al.* reported a 3D cage-based COF with a twofold interpenetrated **acs** net *via* 6-connected organic cages.[38] Our group developed triptycene-based building blocks and synthesized derived frameworks based on **stp**, **ceq**, and **hea** topologies.[39–41] Notably, Yaghi and co-workers presented the pioneering idea to increase the diversity of COFs through higher valency nodes, and a series of BP-COFs were reported in view of 8-connected units and polycubane structures.[42] Nevertheless, these frameworks were only constructed on the basis of the rare $[B_4P_4O_{12}]$ cube, which is defective in stability and functionalization. Therefore, it is highly desired to develop a more general strategy for incorporating high valency in stable COFs, such as imine-linked COFs as one of the most popular members, which is necessary for the extension of structural diversity and potential applications of COFs. However, this avenue is still not quite explored.[43,44]

In this work, we report two 3D microporous and mesoporous imine-linked COFs with **bcu** nets, termed JUC-588 and JUC-589, based on two novel cubic building blocks with different sizes. Both COFs show highly crystalline structures, large surface areas (2728 $m^2\ g^{-1}$ for JUC-588 and 2482 $m^2\ g^{-1}$ for JUC-589), and excellent thermal and chemical stabilities. In addition, the high selectivity of CO_2/N_2 (20 for JUC-588 and 14 for JUC-589) and CO_2/CH_4 (12 for JUC-588 and 10 for JUC-589), promising uptake of H_2 (245 $cm^3\ g^{-1}$ or 2.19 wt% for JUC-588 and 211 $cm^3\ g^{-1}$ or 1.89 wt% for JUC-589 at 77 K and 1 bar), and adsorption of dye molecules for both COFs are studied. Therefore, this study provides a facile strategy for constructing 3D stable COFs with variable pores by enhancing the nodes of building blocks.

Results and discussion

To obtain highly connected knots, we designed two unique building units with eight aldehyde terminal groups, 3,3′,5,5′-tetra(3″,5″-diformylphenyl)-2,2′,6,6′-tetramethoxy-4,4′-dimethyl

State Key Laboratory of Inorganic Synthesis and Preparative Chemistry, Jilin University, Changchun 130012, P. R. China. E-mail: postlh@jlu.edu.cn; xdyao@jlu.edu.cn; qrfang@jlu.edu.cn

† Electronic supplementary information (ESI) available: Materials and characterization, SEM images, TEM images, FT-IR spectra, solid-state ^{13}C NMR spectra, TGA curves, PXRD patterns, gas adsorption, dye adsorption, and unit cell parameters. See https://doi.org/10.1039/d2sc02365b

biphenyl (TDFTD) and 2,3,5,6-tetrakis(([3,5-diformylphenyl]-5-yl)-9*H*-carbazol-9-yl)-1,4-benzenedicarbonitrile (TDFCB, Scheme 1a and b). Due to steric hindrance, both linkers can act as cubic (8-connected) building blocks, which has been proven by single crystals of their analogues.[45,46] Furthermore, because of these building units with distinct sizes, the pores of the obtained frameworks can be regulated. Through the condensation of eight-functional monomers and a linear building unit, 1,4-phenylenediamine (PDA, Scheme 1c), two 3D imine-linked frameworks with microporous or mesoporous channels were synthesized (Scheme 1d and e), which tends to be a **bcu** net based on reticular chemistry (Scheme 1f).[47]

Typically, the syntheses were carried out by suspending PDA and TDFTD or TDFCB in a mixed solution of dioxane and mesitylene in the presence of 3 M acetic acid aqueous solution, followed by heating at 120 °C for 3 days. Morphologies observed by scanning electron microscopy (SEM) and transmission electron microscopy (TEM) demonstrated aggregates of nanoparticles (Fig. S1–S4, ESI†). The formation of imine moieties was verified by Fourier transform infrared (FT-IR) spectra with new vibration peaks at 1630 cm^{-1} for JUC-588 and 1626 cm^{-1} for JUC-589 (Fig. S5, ESI†). Solid-state ^{13}C cross-polarization magic-angle-spinning (CP/MAS) NMR spectroscopy was carried out and illustrated chemical shifts at 160 ppm for JUC-588 and 157 ppm for JUC-589, which further proved the formation of imine bonds (Fig. S6 and S7, ESI†). High thermal stability up to 400 °C for both COFs was confirmed by thermogravimetric analysis (TGA) under a nitrogen atmosphere (Fig. S8 and S9, ESI†). Meanwhile, promising chemical stabilities were evidenced by powder X-ray diffraction (PXRD) patterns after immersing in various solutions for 72 h, such as in acidic (1 M HCl), basic (1 M NaOH), and common organic solvents including dimethylformamide, dichloromethane, tetrahydrofuran, and *n*-hexane (Fig. S10 and S11, ESI†).

For the structure definition of JUC-588 and JUC-589, PXRDs were employed in conjunction with structural simulations (Fig. 1). Model structures were obtained through geometrical energy minimization using the Materials Studio software package on the basis of the **bcu** net.[48] JUC-588 adopted the space group $P4_2/nmc$ (No. 137) with unit cell parameters of $a = b = 23.8190$ Å, $c = 23.9058$ Å, and $\alpha = \beta = \gamma = 90°$, while JUC-589 utilized *Immm* (No. 71) with $a = 35.7099$ Å, $b = 9.7315$ Å, $c = 50.7873$ Å, and $\alpha = \beta = \gamma = 90°$ (Tables S5 and S6, ESI†). The calculated PXRDs of the model crystal structures fitted well with the experimental patterns (Fig. S12 and S13, ESI†). Furthermore, we carried out full profile pattern matching (Pawley) refinement. Peaks at 5.25, 7.39, 8.27, 10.48, 11.7, 14.85, and 15.78 correspond to the (101), (002), (102), (202), (103), (004), and (303) facets of JUC-588, and 3.02, 6.06, 6.96, and 9.09° correspond to the (101), (202), (004), and (303) facets of JUC-589, respectively. The refinement results illustrated good agreement factors ($R_p = 2.86\%$ and $R_{wp} = 3.76\%$ for JUC-588; $R_p = 1.12\%$ and $R_{wp} = 1.53\%$ for JUC-589). Considering these results, both COFs were proposed to have the expected 3D frameworks with the **bcu** net, microporous JUC-588 with a pore size of 1.5 nm and rhombic mesoporous JUC-589 with a pore size of 2.1 nm × 2.4 nm, respectively (Fig. 2).

Subsequently, N_2 adsorption and desorption measurements were carried out at 77 K to determine the permanent channel structures and specific surface areas. As shown in Fig. 3a, JUC-588 demonstrated a sharp increase at low pressure ($P/P_0 < 0.05$), which illustrated the microporous structure with a type I

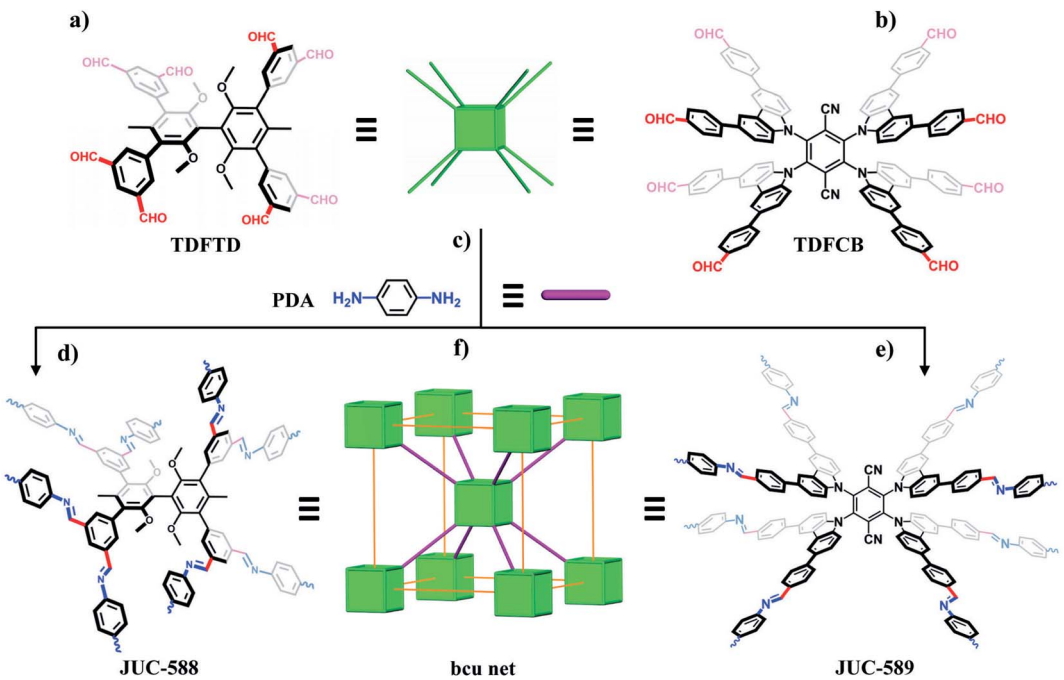

Scheme 1 A strategy for preparing 3D COFs based on cubic building blocks[a]. [a]Molecular structures of TDFTD (a) and TDFCB (b) with cubic (8-connected) knots. Structure of a linear building block, PDA (c). Extended frameworks of JUC-588 (d) and JUC-589 (e). (f) A **bcu** net for JUC-588 and JUC-589.

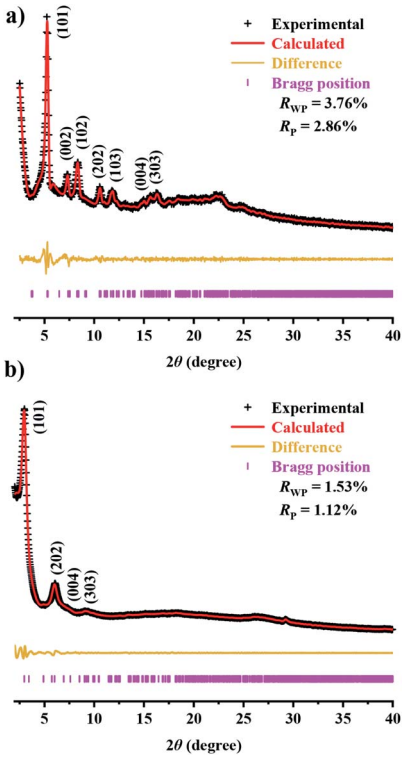

Fig. 1 PXRD patterns of JUC-588 (a) and JUC-589 (b).

isotherm. Different from JUC-588, the nitrogen adsorption of JUC-589 with a type IV isotherm exhibited an extra uptake step between $P/P_0 = 0.1$ and 0.2, proving the mesoporous nature of this framework (Fig. 3b). Based on the Brunauer–Emmett–Teller (BET) model, specific surface areas were calculated to be 2728 $m^2\ g^{-1}$ for JUC-588 and 2482 $m^2\ g^{-1}$ for JUC-589 respectively, which is slightly lower than that (3300 $m^2\ g^{-1}$) of JUC-564 with the largest pore size (43 Å) among 3D COFs and record-breaking low density (0.108 g cm^{-3}) among crystalline materials reported to date (Fig. S14, ESI†).[39] Pore-size distributions were determined by nonlocal density functional theory (NLDFT), in which JUC-588 showed a narrow distribution centered at 1.7 nm (Fig. 3c), while JUC-589 demonstrated the presence of dominant mesopores of about 2.1 nm and 2.3 nm (Fig. 3d). These results were in good agreement with those of the proposed models (1.5 nm for JUC-588 and 2.1 nm × 2.4 nm for JUC-589). Remarkably, JUC-589 represents the first example of mesoporous COFs based on an 8-connected node and shows a higher BET surface area and pore size compared to those of similar materials reported, such as BP-COF-1 (BET: 519 $m^2\ g^{-1}$ and pore size: 0.6 nm),[42] and NUST-5 (BET: 680 $m^2\ g^{-1}$ and pore size: 1.5 nm),[43] and NKCOF-23 (BET: 1900 $m^2\ g^{-1}$ and pore size: 1.7 nm).[44]

For exploring the potential applications of these novel COFs in the fields of energy or the environment, we tested the selectivity of CO_2/N_2 and CO_2/CH_4, storage of H_2, and dye adsorption. The adsorption isotherms of CO_2, N_2 and CH_4 were recorded at 273 K and 1 bar, which can be comparable with those from reported porous materials (Tables S2–S4†). As shown in Fig. 4a and b, the sorption amounts of CO_2 were as high as 67 $cm^3\ g^{-1}$ for JUC-588 and 40 $cm^3\ g^{-1}$ for JUC-589

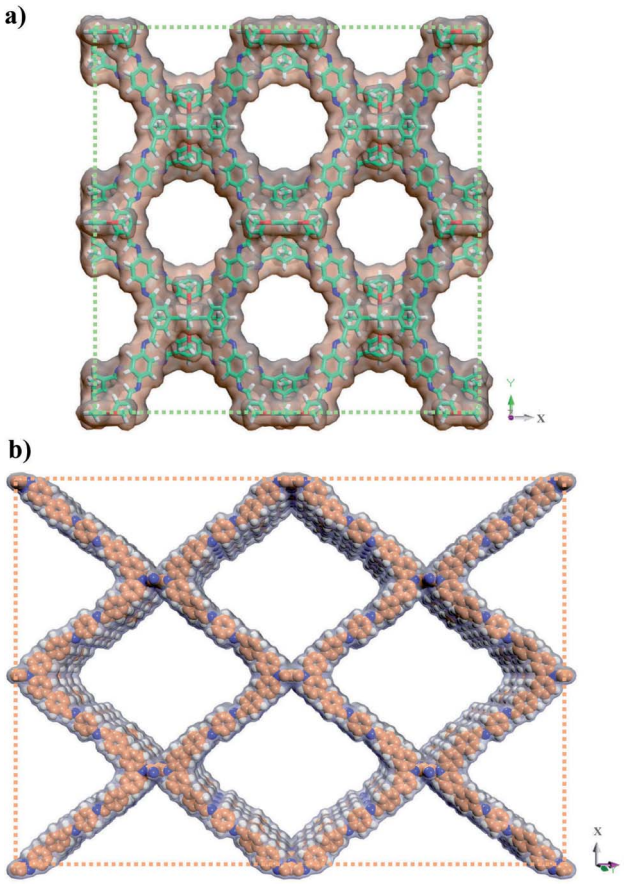

Fig. 2 Structural representations of microporous JUC-588 (a) and mesoporous JUC-589 (b).

respectively, which are much higher than those of other gases, such as CH_4 (16 $cm^3\ g^{-1}$ for JUC-588 and 12 $cm^3\ g^{-1}$ for JUC-589) and N_2 (6 $cm^3\ g^{-1}$ for JUC-588 and 5 $cm^3\ g^{-1}$ for JUC-589). The ideal adsorption selectivity was calculated from the ratio of the initial slopes based on the Henry region of the isotherms (Fig. S15 and S16, ESI†), and high selectivity of CO_2/N_2 (20 for

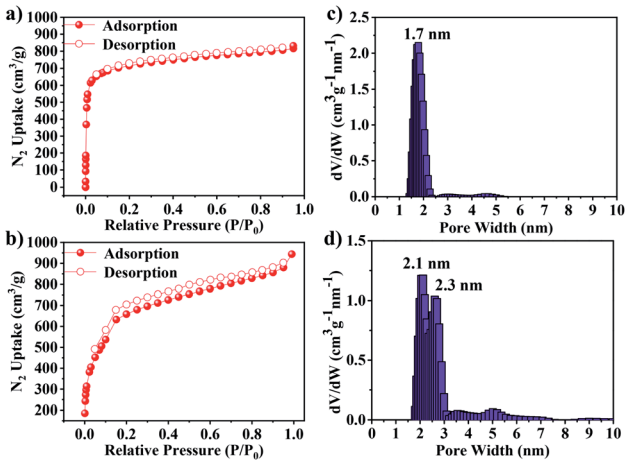

Fig. 3 N_2 adsorption–desorption isotherms at 77 K for JUC-588 (a) and JUC-589 (b). Pore size distribution for JUC-588 (c) and JUC-589 (d).

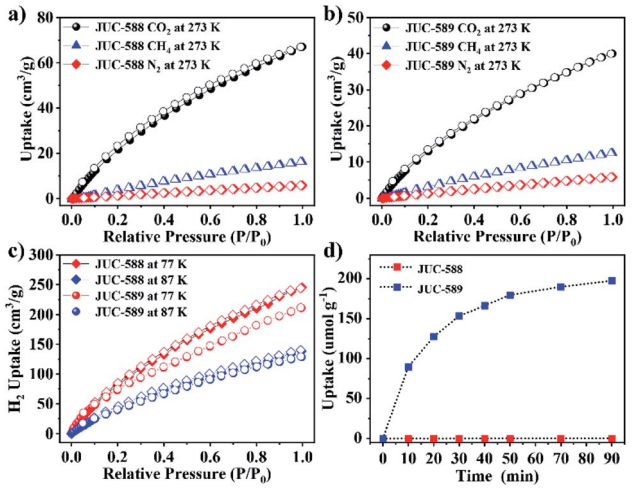

Fig. 4 Adsorption of N_2, CH_4, and CO_2 for JUC-588 (a) and JUC-589 (b) measured at 273 K. (c) Uptake of H_2 for JUC-588 and JUC-589 measured at 77 K and 87 K. (d) Adsorption of a dye molecule for JUC-588 and JUC-589.

JUC-588 and 14 for JUC-589) or CO_2/CH_4 (12 for JUC-588 and 10 for JUC-589) was obtained (Table S1†). Furthermore, the H_2 uptakes of both COFs were explored at different temperatures under 1 atm (Fig. 4c). The H_2 storage capacity of JUC-588 was 245 $cm^3\ g^{-1}$ (or 2.19 wt%) at 77 K and 138 $cm^3\ g^{-1}$ (or 1.23 wt%) at 87 K respectively, which is lower than that of JUC-596 with functional triptycene groups with high fractional free volume and numerous available sites (305 $cm^3\ g^{-1}$ or 2.72 wt% at 77 K);[41] however, it exceeded that of JUC-589 (211 $cm^3\ g^{-1}$ or 1.89 wt% at 77 K and 129 $cm^3\ g^{-1}$ or 1.15 wt% at 87 K) and most porous materials under approximate test conditions, such as PAF-1 (179 $cm^3\ g^{-1}$ or 1.60 wt%),[49] MOF-177 (139 $cm^3\ g^{-1}$ or 1.25 wt%),[50] and CTC-COF (125 $cm^3\ g^{-1}$ or 1.12 wt%).[51] Based on the above results, the isosteric heats of adsorption (Q_{st}) for H_2 were calculated to be 4.12 kJ mol^{-1} for JUC-588 and 6.54 kJ mol^{-1} for JUC-589, respectively (Fig. S17 and S18, ESI†). In addition, mesoporous JUC-589 could effectively adsorb a dye molecule, Coomassie brilliant blue R250 (R250) with dimensions of about 2.1 nm × 1.8 nm × 0.6 nm, while JUC-588 could barely take up the R250 molecule due to its microporous channels, which further proves the existence of mesopores in JUC-589 (Fig. 4d, S19 and S20, ESI†). The maximum uptake capacity of R250 for JUC-589 is about 185.7 mg g^{-1}, which is comparable with those from reported porous materials, such as PCN-124-stu(Cu) (78.7 mg g^{-1})[52] and MIL-100(Fe, Al) (100.0 mg g^{-1}).[53]

Conclusions

In summary, we designed two new monomers with eight aldehyde functional groups, TDFTD or TDFCB, and further assembled their derived 3D imine COFs with rare **bcu** nets, named microporous JUC-588 and mesoporous JUC-589. Both materials showed high crystallinity, large surface areas (up to 2728 $m^2\ g^{-1}$ for JUC-588), and good thermal and chemical stabilities. Furthermore, the selectivity of CO_2/N_2 (20 for JUC-588 and 14 for JUC-589) and CO_2/CH_4 (12 for JUC-588 and 10 for JUC-589), the uptake of H_2 (245 $cm^3\ g^{-1}$ for JUC-588 and 211 $cm^3\ g^{-1}$ for JUC-589 at 77 K and 1 bar), and the adsorption of dye were studied, which indicates the promising potential of these COFs constructed with high valency in the fields of energy and the environment. Therefore, this work develops a general strategy for enriching the structural diversity of COF materials and promotes their potential applications. Furthermore, the nanomorphologies of 3D COFs would be a great topic of research, which will greatly promote their performance in catalysis and separation, and related study is underway.

Data availability

The authors declare that the data supporting the findings of this study are available within the article and its ESI† or from the corresponding author upon reasonable request.

Author contributions

Q. F., X. Y. and H. L. were responsible for the overall design, direction and supervision of the project. L. L. performed the experimental work. X. G., H. Z., Z. Z. and Y. L. took SEM images and helped with the TGA and PXRD tests. L. Z. was in charge of other physical measurements. All authors discussed the results and contributed to the writing of the manuscript.

Conflicts of interest

There are no conflicts to declare.

Acknowledgements

This work was supported by the National Natural Science Foundation of China (22025504, 21621001, 21390394, and 22105082), "111" project (BP0719036 and B17020), China Postdoctoral Science Foundation (2020TQ0118 and 2020M681034), and program for JLU Science and Technology Innovative Research Team.

Notes and references

1 A. P. Côté, A. I. Benin, N. W. Ockwig, M. O'Keeffe, A. J. Matzger and O. M. Yaghi, *Science*, 2005, **310**, 1166.
2 J. W. Colson, A. R. Woll, A. Mukherjee, M. P. Levendorf, E. L. Spitler, V. B. Shields, M. G. Spencer, J. Park and W. R. Dichtel, *Science*, 2011, **332**, 228.
3 X. Feng, X. S. Ding and D. L. Jiang, *Chem. Soc. Rev.*, 2012, **41**, 6010–6022.
4 Y. Yusran, X. Y. Guan, H. Li, Q. R. Fang and S. L. Qiu, *Natl. Sci. Rev.*, 2020, **7**, 170.
5 K. Y. Geng, T. He, R. Y. Liu, S. Dalapati, K. T. Tan, Z. P. Li, S. S. Tao, Y. F. Gong, Q. H. Jiang and D. L. Jiang, *Chem. Rev.*, 2020, **120**, 8814.
6 P. Kuhn, M. Antonietti and A. Thomas, *Angew. Chem., Int. Ed.*, 2008, **47**, 3450.
7 S. S. Han, H. Furukawa, O. M. Yaghi and W. A. Goddard, *J. Am. Chem. Soc.*, 2008, **130**, 11580.

8 Q. R. Fang, Z. B. Zhuang, S. Gu, R. B. Kaspar, J. Zheng, J. H. Wang, S. L. Qiu and Y. S. Yan, *Nat. Commun.*, 2014, **5**, 4503.
9 S. Y. Ding, J. Gao, Q. Wang, Y. Zhang, W. G. Song, C. Y. Su and W. Wang, *J. Am. Chem. Soc.*, 2011, **133**, 19816.
10 V. S. Vyas, F. Haase, L. Stegbauer, G. Savasci, F. Podjaski, C. Ochsenfeld and B. V. Lotsch, *Nat. Commun.*, 2015, **6**, 8508.
11 Q. Sun, B. Aguila, J. Perman, N. Nguyen and S. Q. Ma, *J. Am. Chem. Soc.*, 2016, **138**, 15790.
12 X. R. Wang, X. Han, J. Zhang, X. W. Wu, Y. Liu and Y. Cui, *J. Am. Chem. Soc.*, 2016, **138**, 12332.
13 S. C. Yan, X. Y. Guan, H. Li, D. H. Li, M. Xue, Y. S. Yan, V. Valtchev, S. L. Qiu and Q. R. Fang, *J. Am. Chem. Soc.*, 2019, **141**, 2920.
14 S. Bi, P. Thiruvengadam, S. C. Wei, W. B. Zhang, F. Zhang, L. S. Gao, J. S. Xu, D. Q. Wu, J. S. Chen and F. Zhang, *J. Am. Chem. Soc.*, 2020, **142**, 11893.
15 F. Q. Chen, X. Y. Guan, H. Li, J. H. Ding, L. K. Zhu, B. Tang, V. Valtchev, Y. S. Yan, S. L. Qiu and Q. R. Fang, *Angew. Chem., Int. Ed.*, 2021, **60**, 22230.
16 S. Wan, J. Guo, J. Kim, H. Ihee and D. L. Jiang, *Angew. Chem., Int. Ed.*, 2008, **47**, 8826.
17 M. Dogru, M. Handloser, F. Auras, T. Kunz, D. Medina, A. Hartschuh, P. Knochel and T. Bein, *Angew. Chem., Int. Ed.*, 2013, **52**, 2920.
18 G. H. V. Bertrand, V. K. Michaelis, T. C. Ong, R. G. Griffin and M. Dinca, *Proc. Natl. Acad. Sci. U. S. A.*, 2013, **110**, 4923.
19 H. Li, J. H. Chang, S. S. Li, X. Y. Guan, D. H. Li, C. Y. Li, L. X. Tang, M. Xue, Y. S. Yan, V. Valtchev, S. L. Qiu and Q. R. Fang, *J. Am. Chem. Soc.*, 2019, **141**, 13324.
20 Y. Du, H. S. Yang, J. M. Whiteley, S. Wan, Y. H. Jin, S. H. Lee and W. Zhang, *Angew. Chem., Int. Ed.*, 2016, **55**, 1737.
21 S. Chandra, T. Kundu, S. Kandambeth, R. BabaRao, Y. Marathe, S. M. Kunjir and R. Banerjee, *J. Am. Chem. Soc.*, 2014, **136**, 6570.
22 S. Wang, Q. Y. Wang, P. P. Shao, Y. Z. Han, X. Gao, L. Ma, S. Yuan, X. J. Ma, J. W. Zhou, X. Feng and B. Wang, *J. Am. Chem. Soc.*, 2017, **139**, 4258.
23 X. Y. Guan, H. Li, Y. C. Ma, M. Xue, Q. R. Fang, Y. S. Yan, V. Valtchev and S. L. Qiu, *Nat. Chem.*, 2019, **11**, 587.
24 J. P. Yu, L. Y. Yuan, S. Wang, J. H. Lan, L. R. Zheng, C. Xu, J. Chen, L. Wang, Z. W. Huang, W. Q. Tao, Z. R. Liu, Z. F. Chai, J. K. Gibson and W. Q. Shi, *CCS Chem.*, 2019, **1**, 286.
25 R. R. Liang, F. Z. Cui, R. H. A, Q. Y. Qi and X. Zhao, *CCS Chem.*, 2020, **2**, 139.
26 J. H. Chang, H. Li, J. Zhao, X. Y. Guan, C. M. Li, G. T. Yu, V. Valtchev, Y. S. Yan, S. L. Qiu and Q. R. Fang, *Chem. Sci.*, 2021, **12**, 8452.
27 S. Y. Ding and W. Wang, *Chem. Soc. Rev.*, 2013, **42**, 548.
28 D. Rodriguez-San-Miguel and F. Zamora, *Chem. Soc. Rev.*, 2019, **48**, 4375.
29 S. Kandambeth, K. Dey and R. Banerjee, *J. Am. Chem. Soc.*, 2019, **141**, 1807.
30 S. Mohata, K. Dey, S. Bhunia, N. Thomas, E. B. Gowd, T. G. Ajithkumar, C. M. Reddy and R. Banerjee, *J. Am. Chem. Soc.*, 2022, **144**, 400.
31 A. K. Mahato, S. Bag, H. S. Sasmal, K. Dey, I. Giri, M. Linares-Morear, C. Carbonell, P. Falcaro, E. B. Gowd, R. K. Vijayaraghavan and R. Banerjee, *J. Am. Chem. Soc.*, 2021, **143**, 20916.
32 K. Dey, S. Mohata and R. Banerjee, *ACS Nano*, 2021, **15**, 12723.
33 H. S. Sasmal, S. Bag, B. Chandra, P. Majumder, H. Kuiry, S. Karak, S. S. Gupta and R. Banerjee, *J. Am. Chem. Soc.*, 2021, **143**, 8426.
34 K. Dey, S. Bhunia, H. S. Sasmal, C. M. Reddy and R. Banerjee, *J. Am. Chem. Soc.*, 2021, **143**, 955.
35 Z. S. Xiong, B. B. Sun, H. B. Zou, R. W. Wang, Q. R. Fang, Z. T. Zhang and S. L. Qiu, *J. Am. Chem. Soc.*, 2022, **144**, 6583.
36 X. Y. Guan, F. Q. Chen, Q. R. Fang and S. L. Qiu, *Chem. Soc. Rev.*, 2020, **49**, 1357.
37 O. Yahiaoui, A. N. Fitch, F. Hoffman, M. Froba, A. Thomas and J. Roeser, *J. Am. Chem. Soc.*, 2018, **140**, 5330.
38 Q. Zhu, X. Wang, R. Clowes, P. Cui, L. J. Chen, M. A. Little and A. I. Cooper, *J. Am. Chem. Soc.*, 2020, **142**, 16842.
39 H. Li, J. H. Ding, X. Y. Guan, F. Q. Chen, C. Y. Li, L. K. Zhu, M. Xue, D. Q. Yuan, V. Valtchev, Y. S. Yan, S. L. Qiu and Q. R. Fang, *J. Am. Chem. Soc.*, 2020, **142**, 13334.
40 H. Li, F. Q. Chen, X. Y. Guan, J. L. Li, C. Y. Li, B. Tang, V. Valtchev, Y. S. Yan, S. L. Qiu and Q. R. Fang, *J. Am. Chem. Soc.*, 2021, **143**, 2654.
41 C. Y. Yu, H. Li, Y. J. Wang, J. Q. Suo, X. Y. Guan, R. Wang, V. Valtchev, Y. S. Yan, S. L. Qiu and Q. R. Fang, *Angew. Chem., Int. Ed.*, 2022, **61**, e202117101.
42 C. Gropp, T. Q. Ma, N. Hanikel and O. M. Yaghi, *Science*, 2020, **370**, 424.
43 Z. Shan, M. M. Wu, D. Y. Zhu, X. W. Wu, K. Zhang, R. Verduzco and G. Zhang, *J. Am. Chem. Soc.*, 2022, **144**, 5728.
44 F. Z. Jin, E. Lin, T. H. Wang, S. B. Geng, T. Wang, W. S. Liu, F. H. Xiong, Z. F. Wang, Y. Chen, P. Cheng and Z. J. Zhang, *J. Am. Chem. Soc.*, 2022, **144**, 5643.
45 W. G. Lu, Z. W. Wei, D. Q. Yuan, J. Tian, S. Fordham and H. C. Zhou, *Chem. Mater.*, 2014, **26**, 4589.
46 M. K. Etherington, N. A. Kukhta, H. F. Higginbotham, A. Danos, A. N. Bismillah, D. R. Graves, P. R. McGonigal, N. Haase, A. Morherr, A. S. Batsanov, C. Pflumm, V. Bhalla, M. R. Bryce and A. P. Monkman, *J. Phys. Chem. C*, 2019, **123**, 11109.
47 M. Li, D. Li, M. O'Keeffe and O. M. Yaghi, *Chem. Rev.*, 2014, **114**, 1343.
48 *Materials Studio ver. 7.0*, Accelrys Inc., San Diego, CA.
49 T. Ben, H. Ren, S. Q. Ma, D. P. Cao, J. H. Lan, X. F. Jing, W. C. Wang, J. Xu, F. Deng, J. M. Simmons, S. L. Qiu and G. S. Zhu, *Angew. Chem., Int. Ed.*, 2009, **48**, 9457.
50 H. K. Chae, D. Y. Siberio-Perez, J. Kim, Y. Go, M. Eddaoudi, A. J. Matzger, M. O'Keeffe and O. M. Yaghi, *Nature*, 2004, **427**, 523.
51 J. R. Zhen, S. Y. Ding, W. Wang, J. M. Liu, J. L. Sun, Z. T. Huang and Q. Y. Zheng, *Chin. J. Chem.*, 2016, **34**, 783.
52 W. G. Jin, W. Chen, P. H. Xu, X. W. Lin, X. C. Huang, G. H. Chen, F. S. Lu and X. M. Chen, *Chem.–Eur. J.*, 2017, **23**, 13058.
53 H. Lv, H. Zhao, T. Cao, L. Qian, Y. Wang and G. Zhao, *J. Mol. Catal. A: Chem.*, 2015, **400**, 81.